http://dx.doi.org/10.4314/gjgs.v11.1.7

GLOBAL JOURNAL OF GEOLOGICAL SCIENCES VOL 11, 2013: 73-93
COPYRIGHT© BACHUDO SCIENCE CO. LTD PRINTED IN NIGERIA. ISSN 1596-6798
www.globaljournalseries.com; Info@globaljournalseries.com

GEOCHEMISTRY OF THE BAYONPLUTONIC COMPLEX - WESTERN CAMEROON

ROSE NOEL NGO BELNOUN, JEAN PIERRE TCHOUANKOUÉ, ZENON ITIGA, NICOLE ARMELLE SIMENI WAMBO, SÉBASTIEN OWONA, FRIEDRICH KOLLER AND MARTIN THÖNI

(Received 14May 2013; Revision Accepted 16September 2013)

ABSTRACT

The BayonNeoproterozoic plutonic complex located in Western Cameroon intrudes gneisses of Paleo to Neo Proterozoic age. The complex is composed of gabbro, monzogabbro and monzonites frequently crosscut by trachytic and granitic veins. The primary mineral assemblages of the gabbro and monzogabbro is plagioclase (An_{30} - An_{69}), clinopyroxene (En_{40-42} Fs_{12-18} Wo_{45-47}), hypersthene (En_{62-65} Fs_{34-37} Wo_{1-4}) and orthoclase (Or_{78}-Or_{91}) whilebiotite, magnetite, Ilmenite and apatite constitute accessory minerals. Monzonite is formed of plagioclase (An_{22} to An_{39}), orthoclase (Or_{80}-Or_{87}),clinopyroxene (En_{38-39} Fs_{14-20} Wo_{45-46}), biotite and quartz. Amphiboles occur as secondary minerals. Ilmenite and apatite are accessory minerals in monzonite.The rocks are mafic to intermediate in composition (41 – 61 wt % SiO_2) and transalkaline with high-K and have shoshonitic features. Bayon plutonic rocks have high abundance of Ba, Sr ,V and Zr but possesses low concentrations of Rb, Sc, Y and Th.Gabbroic rocks show moderately fractioned REE patterns (La_N/Lu_N= 14 – 27) with none or negligible Eu anomalies. The monzonite shows also moderate fractionatedpatterns (La_N/Lu_N= 20 – 27) with fairly positive Eu anomalies. All the studied rocks show flat HREE features. The primitive mantle- normalized element patterns are almost homogeneous with negative anomalie in Ta, Nb, Th, P and Ti. Sm/Nd-wr-Cpx-Pl ages of the complex are 580 ± 13 Ma; 553 ± 32 Ma for the monzogabbro and 547 ± 26 Ma for the monzonite. The Nd/Sr isotopic compositions show that the Bayon plutonic rocks were generated by partial melting of subcontinental lithospheric mantle. The depleted mantle Nd model age TD_M of 1.6 – 1.7 Ga indicates that the studied rocks originated by partial melting of Mesoproterozoic mantle.

KEYWORDS: West Cameroon, Panafrican, Pluton, Geochemistry, partial meting

INTRODUCTION

The Bayon plutonic complex belongs to the Neoproterozoic fold belt of Cameroon. This fold belt is associated with the Pan-African tectonothermalevent 650-500 Ma and is related to the collision of the Congo Craton with the West African Craton (Fig.1a). That collision structured the Pan-African North Equatorial belt which extends in Sudan, Central African Republic, Cameroon and through correlations with North-East Brazil (*Castaing et al., 1994; Nzenti et al., 1998; Toteu et al.,2001; Abdelsalam et al., 2002; Oliveira et al., 2006*).In West Cameroon, Pan-African massifsare widely distributed (Fig.1b) andare described as syn to post–collisional, calc-alkaline, ferro-potassic and metaluminous(*Tchouankoue, 1992; Nguiessi et al.,1997; Tagne – Kamga, 2003; Nzolang et al., 2003; Tetsopgang, 2003; Djouka Fonkwe et al., 2008*).According to available ages, the massifswere emplaced during the Pan – African D2 deformation event. The emplacement age (Rb – Sr whole rock and Th –U – Pb methods) are between 720-540 Ma (*Toteu et al., 1990;Tchouankoue, 1992; Nguiessi et al., 1997; Tagne – Kamga, 2003; Nzolang et al., 2003; Tetsopgang, 2003; Djouka Fonkwe et al., 2008; Njiekak et al., 2008., Tchaptchet Tchato et al., 2009; Kwekam et al., 2010*). Plutonic rocks in Bayon area in the southwestern part of the Cameroon orogenic belt havenot yet been investigated in detail. In this paper we reportthe geochemistry of the Bayon plutonic complex,

Rose Noel Ngo Belnoun, Department of Earth Sciences, University of Yaoundé I, P.O. Box 812, Yaoundé Cameroon.
Jean Pierre Tchouankoué, Department of Earth Sciences, University of Yaoundé I, P.O. Box 812, Yaoundé Cameroon.
Zenon Itiga,Institute of Geological and Mining Research, P.O. Box 4110, Yaoundé, Cameroon.
Nicole Armelle Simeni Wambo, Department of Earth Sciences, University of Ngaoundere, P.O. Box 454, Ngaoundere, Cameroon.
Sébastien Owona,Department of Earth Sciences, University of Douala, P.O. Box 24157, Douala, Cameroon.
Friedrich Koller, Department of Lithospheric Research, University of Vienna, Althanstrasse 14, P.O. Box 1090 Vienna, Austria.
Martin Thöni, Department of Lithospheric Research, University of Vienna, Althanstrasse 14, P.O. Box 1090 Vienna, Austria.

and discusstheir significance in the framework of the Panafrican orogeny in Cameroon.

Regional geological setting

The Pan-African fold belt in Cameroon is divided into three structural domains: (Southern domain; Central domain and Northern domain (*Nzenti et al., 1994; Ngnotue et al., 2000, Toteu et al., 2004*): The Southern domain (Yaounde) is thrusted onto the Archaean Congo Craton towards the South (*Nédelec et al., 1986*); The Central domain(Adamawa) is a huge domain located between the Sanaga Fault in the south and the AdamawaShear Zone (ASZ) to the North and the Northern domain is located to the West of the ASZ and extends along the western border of Cameroon. The Proterozoic includes: (1) the palaeoproterozoic, represented by the Nyong series and considered as the Cameroonian part of the West Central African Fold Belt (*Feybesse et al., 1998, Penaye et al., 2004*); (2) the Neoproterozoic represented by the Pan-African North Equatorial and Post-tectonic granitoids (*Nzenti et al., 1998; Toteu et al., 2004; Mwondo et al., 2007, Owona et al., 2011b*). The Bayon plutoniccomplex belongs tothe Western Cameroon Supergroup –WCSG (Fig. 1a, Owona et al., 2012b). The WCSG has been affected by the Pan-African polyphasedeformation and associated with magmatic episodes from 750-500Ma(*Toteu et al.,* 1990*;Tchouankoue, 1992; Nguiessi et al.,*1994;*Nzolang et al., 2003;Djouka Fonkwe et al., 2008; Njiekak et al., 2008; Tchaptchet Tchato et al., 2009).*The WCSG is also affected by the Central Cameroon Shear Zone (*Ngako et al., 2003; Njonfang et al., 2008; Njanko et al., 2010;Kwekam et al., 2010*)

The emplacement of the Bayon plutonic complex like other granitoids in West Cameroon was controlled not only by a N30°E strike-slip shear zone, forming a prolongation of the Cameroon Volcanic Line, but also by the N70°E central Cameroon shear zone. Both directions of shear zones are characterized by schistosity and foliation, fault orientations and the alignment of the massifs. Geologically, the Bayon plutonic complex (Fig.1b, 1c) is emplaced within the Paleoproterozoic and Neoproterozoic gneisses which crop out along its northern and eastern border (*TchaptchetTchato et al., 2009*). It is overlain by Tertiary volcanic rocks (basalts) in the southern and south-western parts. The contact with surrounding gneisses is characterized by fractures. The main features are the presence of granitic and trachytic veins which crosscut the intrusion. Based on lithological features, two main lithological groups have been distinguished (Ngo Belnoun, 2008):gabbroic rocks (gabbroand monzogabbro) and monzonite.

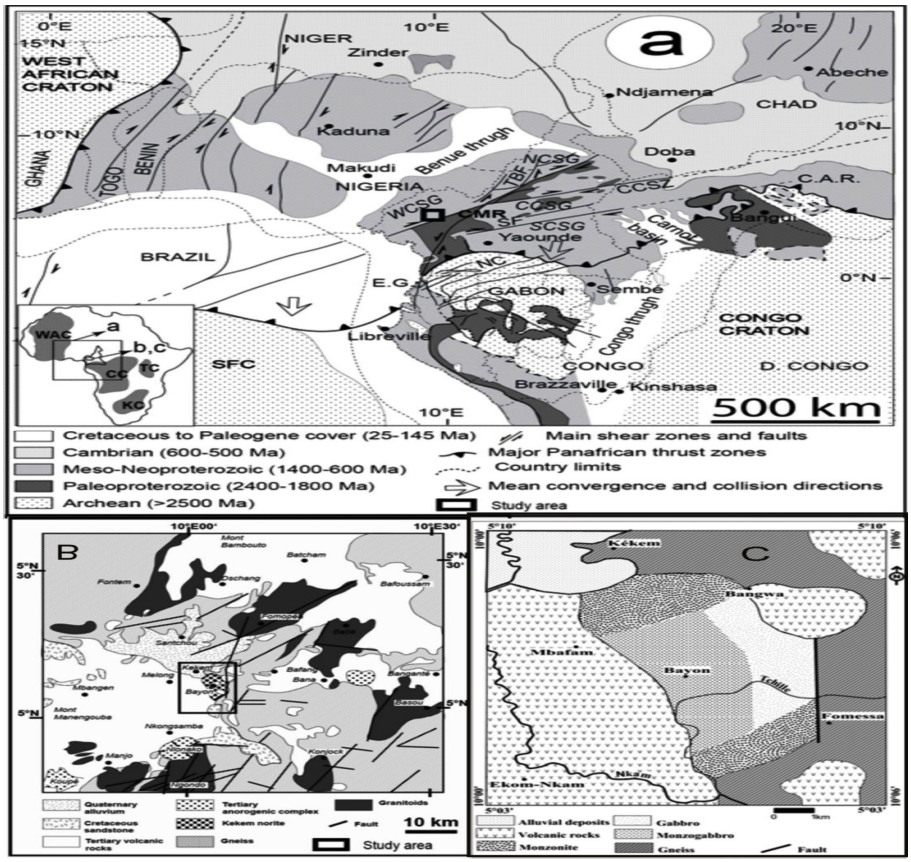

Fig. 1: (a) Geological sketch of the West-Central Africa and South America connection with cratonic masses and the Pan-African province of the Pan-Gondwana belt in a Pangea reconstruction from *Owona et al.* (2012)modified after *Castaing et al.* (1994) and *Ngako et al.* (2003). CMR: Cameroon; CAR: Central African Republic; EG: Equatorial Guinea, NCSG: Northern Cameroon Supergroup; CCSG: Central Cameroon Supergroup; SCSG: Southern Cameroon

Supergroup; WCSG: Western Cameroon Supergroup; CCSZ: Central Cameroon Shear Zone; SF: Sanaga Fault, Tcholieré-Banyo fault. Dashed lines mark the country boundaries. (b) WCSG partial geological map of the Kekem plutonic complex (after Dumort, 1986). (c) :Geological map of the Bayon plutonic complex *(Ngo Belnoun, 2008).*

Analytical methods

Representative samples (0.5-1kg) were collected for electron microprobe (EMP), major and trace element and isotopic data analyses. Analyses were performed at the Department of Lithospheric Sciences and the Centre for Earth Sciences (Laboratory of Geochronology), University of Vienna (Austria).For mineral compositions, polished carbon-coated thin sections were analyzed with a Camera SX-100 electron-microprobe. The operating conditions were four wavelength-dispersive spectrometers; 15 kV accelerating voltage and 20 nA beam current; 1µm beam diameter were used for pyroxenes whereas 5 µm beam were used for feldspars. Major and trace element were analysed by X-ray fluorescence (XRF) spectrometry on fused powder discs using a Phillips PW 2400. Rare earth elements (REE) were done by ICP-MS method with a Perkin Elmer ELAN 6100 DRC.

Isotopic data were obtainedat the Laboratory of Geochronology, Centre for Earth Sciences, University of Vienna. For whole rock (wr) and bulk mineral analysis, the kg-sized samples were cleaned and crushed, and then representative wr splits were taken. Apatite was concentrated using a Wilfley table. Pure mineral separates used for Sm-Nd analysis weighed between 25 and 30 mg.Sample digestions for Sm-Nd analysis was performed in Savillex® beakers using an ultrapure 5:1 mixture of HF and $HClO_4$ for 10 days at 110 °C on a hot plate. Upon cooling, between 5 and 10 % of the sample solution was split off and spiked for Sm and Nd concentration determination by isotope dilution (ID) using a mixed REE tracer (^{147}Sm-^{150}Nd spike). A ^{143}Nd/^{144}Nd ratio of 0.511846±0.000003 (n = 38) and a^{87}Sr/^{86}Sr ratio of 0.710248±0.000002 (n = 18) were determined for the La Jolla (Nd) and the NBS987 (Sr) international standards, respectively, during the period of investigation. Within-run mass fractionation for Nd and Sr isotope compositions (IC) were corrected relative to ^{146}Nd/^{144}Nd = 0.7219, and ^{86}Sr/^{88}Sr = 0.1194, respectively. Uncertainties on the Nd and Sr isotope ratios were quoted as $2\sigma_m$. For the ^{147}Sm/^{144}Nd and the ^{87}Rb/^{86}Sr ratios, a mean error of ±1 % was estimated, including blank contribution, uncertainties on spike composition, and machine drift; regression calculation was based on these uncertainties and the isochron calculations followed Ludwig (2003). Age calculations were based on a decay constant of 6.54 x 10^{-12} a^{-1} for ^{147}Sm *(Lugmair & Marti, 1978)*and 1.42 x 10^{-11} a^{-1} for ^{87}Rb *(Steiger & Jäger, 1977)*; age errors were given at the 2σ level.A ^{143}Nd/^{144}Nd ratio of 0.511846±0.000003 (n = 38) and a ^{87}Sr/^{86}Sr ratio of 0.710248±0.000002 (n = 18) were determined for the La Jolla (Nd) and the NBS987 (Sr) international standards, respectively, during the period of investigation. Within-run mass fractionation for Nd and Sr isotope compositions (IC) were corrected relative to ^{146}Nd/^{144}Nd = 0.7219, and ^{86}Sr/^{88}Sr = 0.1194, respectively. Uncertainties on the Nd and Sr isotope ratios were quoted as $2\sigma_m$. For the ^{147}Sm/^{144}Nd and the ^{87}Rb/^{86}Sr ratios, a mean error of ±1 % was estimated, including blank contribution, uncertainties on spike composition, and machine drift; regression calculation was based on these uncertainties and the isochron calculations followed Ludwig (2003). Age calculations were based on a decay constant of 6.54 x 10^{-12} a^{-1} for ^{147}Sm *(Lugmair & Marti, 1978)* and 1.42 x 10^{-11} a^{-1} for ^{87}Rb *(Steiger & Jäger,* 1977);age errors were given at the 2σ level. For Nd, a continuous depletion of the upper mantle was assumed throughout geological time using the following Depleted Mantle (DM) model parameters: ^{147}Sm/^{144}Nd = 0.222, ^{143}Nd/^{144}Nd = 0.513114 *(Michard et al., 1985)*.

Petrography and Mineralogy

The Bayon plutonic complex (Fig.1c) is made up of gabbroic rocks (alkali-gabbro, syenogabbroand monzogabbro) and monzonite. Alkali gabbro and syenogabbro are considered as Gabbro(sensulato).Representative mineral chemistry data from the three groups of Bayon plutonic complex are given in Table 1.

Gabbro

The gabbro is exposed in the West of the complex in contact with the monzogabbro. It is sometimes crosscut by granitic veins; they are rich in Fe-Ti oxides. The Gabbro(Fig.2a) shows a cumulative texture, with automorphic to subautomorphic fine – coarse crystals Plagioclase(An_{64}- An_{69}) forms the main primary mineral. The modal content of plagioclase is 50 - 55 vol % and occurs as subhedral, rounded crystals. Some anhedral plagioclase crystals portray inclusion of apatite, zircon and iron oxides. Pyroxenes are represented by clinopyroxene (Fig.2b) [augite (En_{41-42} $Fs_{13-18}Wo_{39-45}$), diopside (En_{40-42} $Fs_{12-13}Wo_{45-47}$), and pigeonite ($En_{61-62}Fs_{32}Wo_{6-7}$)] and clinoenstatite ($En_{62-65}Fs_{34-37}Wo_{1-4}$). Clinopyroxenes are subeuhedral. In most samples, they are replaced by brown-green biotite or amphibole (Fig.2c). Apatite occurs as inclusions in feldspars and pyroxene or isolated in the groundmass. Iron oxides (magnetite and ilmenite) are commonly associated with pyroxene.

Monzogabbro

The Monzogabbro occupy large domain of the area. They are the most ubiquitousrock in the area. They are surrounded by gabbro and in some placescrosscut by pegmatitic granite veins and small trachytic veins. They are fine to coarse grained. The rocks show heterogranular to granular texture(Fig.2d). Plagioclase (An_{30}-An_{58}) is thedominant mineral (35 - 40 vol %), and appears either as automorphic to subautomorphic phenocrysts with apatite, biotite and opaque inclusion; or automorphic small crystals often included in K-feldspars. Myrmekite appears in some crystals(Fig.2e). Orthoclase (Or_{84}-Or_{91}) forms automorphic plates and are dominantly perthitic and

poikilitic with clinoenstatite, apatite and ilmenite inclusions.Feldspathoidsusually

show cracks(Fig.2e). Xenomorphic coarse crystals of biotite are poikilitic (Fig.2f), frequently associated with pyroxenes and Fe-Ti oxides. The clinopyroxenes forming about 10 vol% of the rocks consist mostly of augite (En_{39-42} $Fs_{14-17}Wo_{42-44}$)and diopside (En_{42-49} $Fs_{13-15}Wo_{46}$). The coarse grains are subhedral and usually associated with biotite. Glomerophyric association of augite-plagioclase is sparse in all samples. Orthopyroxene (clinoenstatiteEn_{55-63} $Fs_{33-40}Wo_{1-2}$) is the most abundant pyroxene; it occurs as acicular small euhedral crystals associated with biotite. The largest crystals of orthopyroxene show small inclusions of plagioclase, biotite, Fe-Ti oxides, and apatite. A few quartz crystals are also found as inclusions in plagioclase, biotite and orthoclase phenocrysts. Magnetite is the dominant oxide, with minor ilmenite. Zircon appears as inclusions in biotite and apatite appears as prism in the groundmass or as inclusions in the plagioclase.

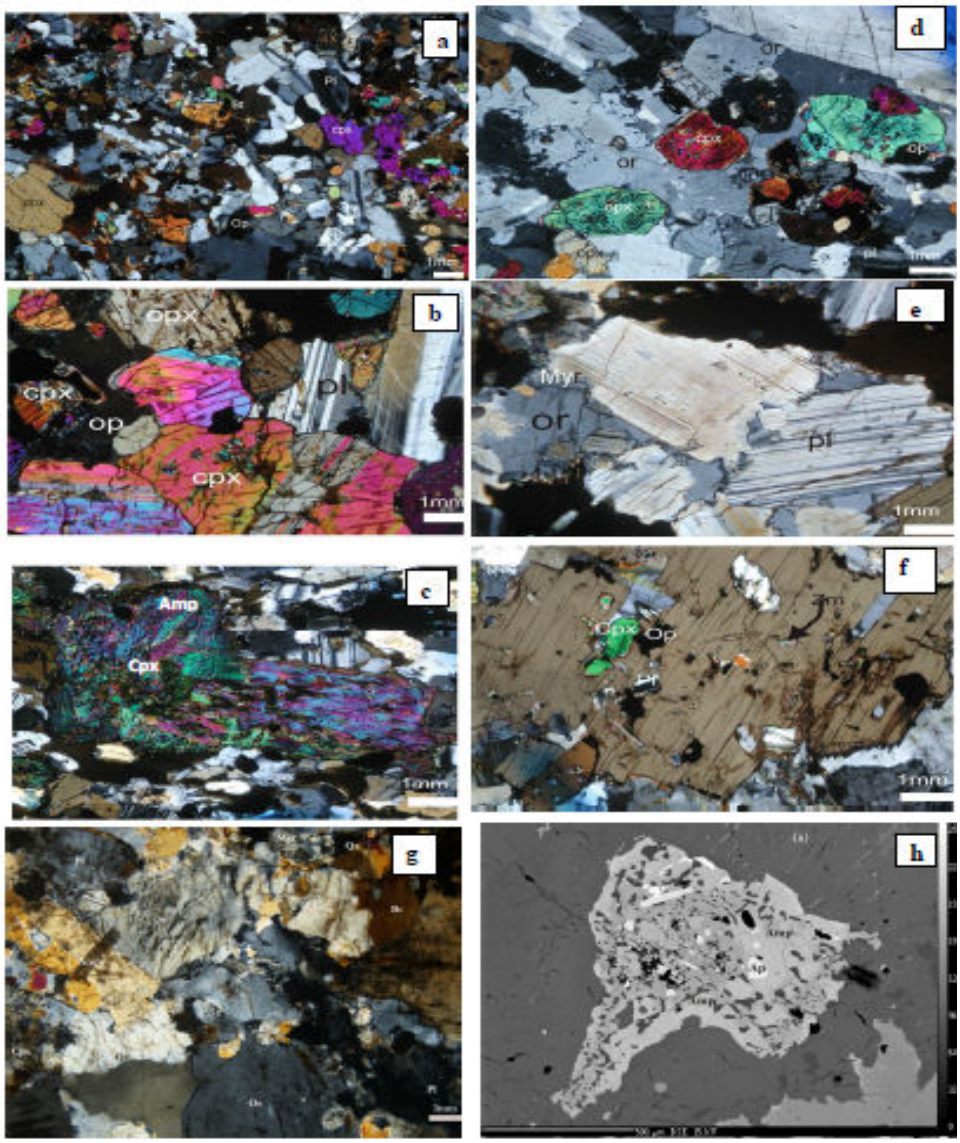

Fig. 2a) Photomicrographs (crossed polars) from gabbro, b)The twinning of Augite and the contact between Orthopyroxene-Clinopyroxene in gabbro; Fe-Ti rimming clinopyroxene are also obvious. f) Gabbro showing pseudomorph of hornblende after pyroxene. d) Photomicrographs (crossed polars) from monzogabbro. e) Feldspars crystals from monzogabbro cracked and fissured; we note also the presence of myrmekites. f) Poikilitic lamella biotite with inclusion of plagioclase, apatite, oxide opaque, Zircon and clinopyroxene in monzogabbro. g) Photomicrographs (crossed polars) from monzonite. h) Back-scattered electron image of monzonite showing replacing pyroxene by amphibole.

Table 1: Chemical composition of feldspars and pyroxenes from Bayon plutonic complex

Feldspar																							
Rocks	Gabbro						Monzogabbro											Monzonite					
Sampe	Pl	Pl	Pl	Pl	Pl	Pl	Pl	Pl	Pl	Pl	Pl	K-feldsp	K-feldsp	K-feldsp	K-feldsp	K-feldsp	K-feldsp	Pl	Pl	Pl	K-feldsp	K-feldsp	K-feldsp
SiO2	51.83	56.22	55.76	57.21	55.76	56.74	60.25	60.06	53.54	59.57	55.53	63.43	63.03	62.87	62.41	64.16	63.26	62.75	59	58.4	63.5	63.55	63.52
TiO2	0.03	0	0.01	0.04	0.01	0.05	0.02	0.02	0.07	0.02	0.06	0.06	0	0.04	0.02	0.05	0.02	0	0	0.01	0.02	0.04	0.01
Al2O3	26.67	23.4	23.82	21.63	23.82	22.84	25.49	25.49	29.45	25.42	27.88	19.22	19.15	19.39	19.32	19.62	19.4	23.01	25.45	25.76	18.46	18.56	18.53
FeO	0.16	0.13	0.19	0.09	0.19	0.15	0.09	0.18	0.12	0.07	0.38	0.08	0.12	0.13	0.03	0.03	0.05	0.14	0.08	0.03	0.04	0.05	0.03
MnO	0	0.01	0.02	0.08	0.02	0	0	0.02	0	0	0.01	0	0.01	0	0	0	0	0	0	0	0	0	0
MgO	0	0	0	0	0	0	0	0	0	0	0	0	0	0.01	0	0.02	0	0.01	0	0	0	0	0
CaO	12.81	9.38	10.15	8.57	10.15	8.8	6.33	6.41	11	6.17	9.46	0.06	0.07	0.04	0.05	0.17	0.11	4.81	7.62	8.07	0.02	0.02	0
Na2O	3.88	6	5.73	6.31	5.73	6.12	7.92	7.97	4.65	7.61	5.94	1.35	1.65	1.37	0.85	2.17	1.61	8.84	7.19	6.76	1.68	2.03	1.34
K2O	0.11	0.2	0.21	0.15	0.21	0.26	0.11	0.21	0.14	0.21	0.22	14.47	13.94	14.2	14.6	12.89	13.85	0.2	0.19	0.17	13.82	13.19	14.18
NiO	0	0	0	0.01	0	0.02	0	0	0	0.03	0	0	0	0	0	0	0		0	0	0.01	0	0
BaO	0.04	0.02	0.01	0	0.01	0	0	0	0	0	0	0	0	0.96	0.92	0	0	0	0	0	0	0	0
Total	95.54	95.36	95.9	94.09	95.9	94.98	100.22	100.36	98.97	99.1	99.47	98.67	97.97	99	98.2	99.11	98.3	99.76	99.52	99.19	97.54	97.44	97.61
A	2.866	2.838	2.827	2.875	2.827	2.848	2.666	2.661	2.746	2.7	2.714	2.799	2.814	2.806	2.837	2.776	2.805	2.67	2.7	2.71	2.83	2.83	2.83
Si	2.472	2.655	2.623	2.737	2.623	2.69	2.674	2.661	2.447	2.677	2.508	2.955	2.952	2.936	2.947	2.965	2.954	2.79	2.65	2.64	2.99	2.99	2.99
Ti	0.001	0	0.001	0.001	0.001	0.002	0.001	0.001	0.002	0.001	0.002	0.002	0	0.001	0.001	0.002	0.001	0	0	0	0	0	0
Al	1.499	1.303	1.321	1.22	1.321	1.276	1.333	1.331	1.586	1.346	1.484	1.055	1.057	1.067	1.075	1.068	1.068	1.2	1.35	1.37	1.02	1.03	1.03
Fe	0.006	0.005	0.007	0.004	0.007	0.006	0.003	0.007	0.004	0.002	0.014	0.003	0.005	0.005	0.001	0.001	0.002	0.01	0	0	0	0	0
Mn	0	0	0.001	0.003	0.001	0	0	0.001	0	0	0	0	0	0	0	0	0	0	0	0	0	0	0
Mg	0	0	0	0	0	0	0	0	0	0	0	0	0	0.001	0	0.001	0	0	0	0	0	0	0
Ca	0.654	1.184	1.201	1.109	1.201	1.16	0.301	0.304	0.539	0.297	0.458	0.003	0.004	0.002	0.002	0.008	0.005	0.23	0.37	0.39	0	0	0
Na	0.359	0.55	0.522	0.586	0.522	0.563	0.682	0.684	0.412	0.663	0.52	0.122	0.149	0.125	0.078	0.195	0.146	0.76	0.63	0.59	0.15	0.19	0.12
K	0.007	0.012	0.013	0.009	0.013	0.016	0.006	0.012	0.008	0.012	0.012	0.86	0.833	0.846	0.88	0.76	0.825	0.01	0.01	0.01	0.83	0.79	0.85
Ni	0	0	0	0	0	0.001	0	0	0	0.001	0	0	0	0	0	0	0	0	0	0	0	0	0
Ba	0.001	0	0	0	0	0	0	0	0	0	0	0	0	0.018	0.017	0	0	0	0	0	0	0	0
Total	5	5.71	5.689	5.669	5.689	5.713	5	5	5	5	5	5	5	5	5	5	5	5	5	5	5	5	5
Or	**0.664**	**0.684**	**0.729**	**0.528**	**0.729**	**0.918**	**0.625**	**1.183**	**0.838**	**1.217**	**1.26**	**87.341**	**84.484**	**86.987**	**91.657**	**78.896**	**84.524**	**1.1**	**1.07**	**0.99**	**84.37**	**80.93**	**87.44**
Ab	**35.19**	**31.493**	**30.1**	**34.38**	**30.1**	**32.36**	**68.939**	**68.407**	**43.003**	**68.221**	**52.513**	**12.376**	**15.157**	**12.806**	**8.09**	**20.24**	**14.931**	**76.04**	**62.4**	**59.67**	**15.55**	**18.97**	**12.56**
An	**64.15**	**67.823**	**69.17**	**65.09**	**69.17**	**66.73**	**30.436**	**30.41**	**56.159**	**30.562**	**46.227**	**0.283**	**0.359**	**0.207**	**0.253**	**0.864**	**0.545**	**22.86**	**36.52**	**39.34**	**0.08**	**0.1**	**0**

The feldspar chemical composition of all rocks is calculated on the basis of eight oxygen; fixing the total number of cation to 5. The structural formulae of pyroxene are calculated on the basis of six oxygen's fixing the total numbers of cation to 4. The structural formulae of ferric and ferrous iron contents were calculated on the basis of stoichiometry using the method of *Lindsley (1983)*

Table 1:(continued)

Pyroxene																
Rocks	Gabbro								Monzogabbro						Monzonite	
Sample	Cpx	Cpx	Cpx	Cpx	Cpx	Opx	Opx	Opx	Cpx	Cpx	Cpx	Cpx	Opx	Opx	Cpx	Cpx
SiO2	51.81	51.81	52.37	51.37	51.84	52.45	52.51	52.43	50.2	50.96	50.25	50.37	52.48	52.49	50.34	50.96
TiO2	0.38	0.38	0.26	0.24	0.33	0.23	0.19	0.09	0.61	0.52	0.66	0.58	0.21	0.15	0.42	0.52
Al2O3	1.68	1.68	1.14	1.16	2.22	0.98	0.72	0.57	2.96	2.58	2.42	1.89	0.86	0.82	1.88	2.58
Cr2O3	0.01	0.01	0.05	0.04	0	0.02	0	0	0.05	0.31	0.04	0.06	0.02	0	0.03	0.31
FeO	10.51	10.51	7.83	7.7	8.14	22.42	21	21.41	9.36	8.5	8.91	9.54	21.92	22.14	9.62	8.5
MnO	0.53	0.53	0.29	0.3	0.49	0.71	0.74	0.73	0.25	0.24	0.32	0.23	1.11	1.06	0.29	0.24
MgO	14.85	14.85	14.89	14.83	13.52	21.94	23.46	23.25	13.39	13.82	13.36	13.41	22.93	22.71	13.91	13.82
CaO	18.98	18.98	22.66	22.39	23.16	0.59	1.02	0.7	21.8	22.37	22.21	22.04	0.74	0.74	21.43	22.37
Na2O	0.25	0.25	0.24	0.33	0.6	0	0	0	0.57	0.65	0.29	0.45	0	0.02	0.46	0.65
K2O	0	0	0	0	0.04	0	0	0	0.02	0.02	0.01	0	0.01	0	0	0.02
TOTAL	99.02	99.02	99.76	98.36	100.35	99.34	99.64	99.2	99.2	99.97	98.52	98.56	100.3	100.14	98.41	99.97
T2	2.265	2.265	2.243	2.277	2.241	2.258	2.242	2.254	2.274	2.251	2.288	2.293	2.238	2.243	2.294	2.251
Si	1.953	1.953	1.955	1.947	1.933	1.971	1.959	1.967	1.9	1.909	1.914	1.922	1.955	1.96	1.922	1.909
Al^{4+}	0.047	0.047	0.045	0.052	0.067	0.029	0.032	0.025	0.1	0.091	0.086	0.078	0.038	0.036	0.078	0.091
Al^{6+}	0.028	0.028	0.005	0	0.031	0.014	0	0	0.032	0.023	0.022	0.007	0	0	0.007	0.023
Fe^{3+}	0.023	0.023	0.061	0.095	0.093	0.003	0.06	0.054	0.111	0.115	0.07	0.103	0.06	0.057	0.118	0.115
Cr	0	0	0.002	0.001	0	0	0	0	0.001	0.009	0.001	0.002	0.001	0	0.001	0.009
Ti	0.011	0.011	0.007	0.007	0.009	0.006	0.005	0.003	0.017	0.015	0.019	0.017	0.006	0.004	0.012	0.015
Fe^{2+}	0.308	0.308	0.182	0.147	0.158	0.701	0.592	0.615	0.183	0.149	0.212	0.199	0.619	0.631	0.186	0.149
Mn	0.017	0.017	0.009	0.01	0.015	0.023	0.023	0.023	0.008	0.008	0.01	0.007	0.035	0.034	0.009	0.008
Mg	0.835	0.835	0.829	0.838	0.751	1.229	1.305	1.3	0.756	0.772	0.759	0.763	1.273	1.264	0.792	0.772
Ca	0.767	0.767	0.906	0.909	0.925	0.024	0.041	0.028	0.884	0.898	0.906	0.901	0.029	0.03	0.877	0.898
Na	0.019	0.019	0.018	0.024	0.043	0	0	0	0.042	0.047	0.021	0.033	0	0.001	0.034	0.047
K	0	0	0	0	0.002	0	0	0	0.001	0.001	0.001	0	0	0	0	0.001
TOTAL Cation	4.007	4.007	4.019	4.03	4.029	4.001	4.017	4.015	4.035	4.036	4.022	4.032	4.017	4.016	4.037	4.036
$Mg/(Mg+Fe^{2+})$	0.73	0.73	0.82	0.851	0.826	0.637	0.688	0.679	0.805	0.838	0.781	0.793	0.673	0.667	0.81	0.838
Wo	**38.961**	**38.961**	**45.196**	**44.942**	**46.561**	**1.202**	**2.026**	**1.384**	**44.569**	**45.15**	**45.801**	**44.91**	**1.461**	**1.471**	**43.49**	**45.152**
En	**42.413**	**42.413**	**41.333**	**41.414**	**37.813**	**62.081**	**64.564**	**64.373**	**38.108**	**38.83**	**38.341**	**38.012**	**63.127**	**62.682**	**39.26**	**38.826**
Fs	**17.686**	**17.686**	**12.59**	**12.437**	**13.439**	**36.716**	**33.411**	**34.242**	**15.201**	**13.64**	**14.778**	**15.413**	**35.413**	**35.777**	**15.55**	**13.636**

Monzonite

A monzonite body occurs in the north and the south of the gabbroic rocks and shows heterogranular to granular texture. The monzonite (Fig.2g)is made up of plagioclase, K- feldspar (orthoclase), clinopyroxene, biotite and quartz. Accessory minerals include titanite, zircon, apatite, opaque minerals. Amphibole occurs as secondary mineral. The feldspar in monzonite is dominated by the presence of euhedral to subhedral tabular plagioclase phenocrysts (An_{22}-An_{39}) (25-40 vol. %), sometimes weakly zoned and partially resorbed into sericite. Euhedral K-feldspar (Or_{80}-Or_{87}) usuallyshows cracks.Some crystals contain euhedral to subhedral inclusions of plagioclase or albite lamellae and others have perthitic intergrowths. Clinopyroxenes have a weak pale yellow green pleochroism. In term of composition, they are diopside (En_{38-39} $Fs_{14-15}Wo_{45-46}$) and augite. (En_{38-39} $Fs_{15-20}Wo_{39-45}$) (Table1).Some clinopyroxenes are completely replaced by amphibole (Fig.2h), in some samples and are recognizable only by their characteristic morphology. Biotite (20 vol %), in monzonite is ferroan. Itis the most mafic mineral in the monzonite with a strong reddish brown-yellowish brown pleochroism. They occur as poikilitic plates with inclusion of apatite, Ilmenite and zircon, or insmall flakes. Quartz (8 vol %) forms subeuhedral and polygonal crystals with undulatory extinction. Iron oxides represented by ilmenite and magnetite occur as inclusion in pyroxene.

Geochemistry

Representative chemicaldata of eighteen samples from Three groups of Bayon plutonic complex are given in Table 2.

GEOCHEMICAL FEATURES

Majors elements

Major elements for Bayon plutonic rocks are shown in the selected oxide diagrams(Fig.3).The gabbro shows basic composition (SiO_2= 41 – 48.62 wt%). It has high Al_2O_3 content (12.99-16.79 wt %), Fe_20_3 ranges from11.63 wt% -14.80 wt%, CaOfrom 7.89 wt %-10.85 wt % whilst TiO_2 content ranges from 1.86 wt %-2.24 wt %. The high value for TiO_2 could be explained by the abundance of ilmenite in the sample. MgO content varies from 5.13 wt % to 9.23 wt %, MnO is not greater than 0.2 wt% and P_2O_5varied from 0.63 wt % to 1.37 wt%. The monzogabbro is intermediate (SiO_2= 50.71-56.70 wt%) and have high content of Al_2O_3(13.81-19.82 wt %), Fe_20_3(7.00-9.11wt%), CaO(5.52 wt %-7.93 wt %). The monzonite is intermediate in composition (SiO_2= 59.58 – 61.06 wt%) with highAl_2O_3(15.36-18.27 wt %) and K_2O(4.24 wt %-5.63 wt %). K_2O/Na_2O ratio ranges from 0.15-1.37. The Bayonplutonic rocks have a high total alkali content (5.47 wt %< Na_2O+K_2O<9.73wt %). In the plutonic total alkali vs silica (TAS) diagram (Fig.4a), the rocks can be classified as transalkaline rocks; there exists a gap between 56.70 and 59.58 % SiO_2 and this separates the gabbroic rocks from monzonite. When considering K_2O vs SiO_2(Fig. 4c), all the analysed samples have high-K calc-alkaline to shoshonite character. The diagram ofFrost et al., 2001(Fig. 4b) clearlyindicates that the rocks are magnesian. The Al saturation index was used by Chappell and White (1992)to discriminate the I-type (A/CNK < 1.1) and S-type granites (A/CNK > 1.1). All the studied rocks have A/CNK= 0.52-1.07 and belong to theI-type granite. They are metaluminous (Fig. 4d).

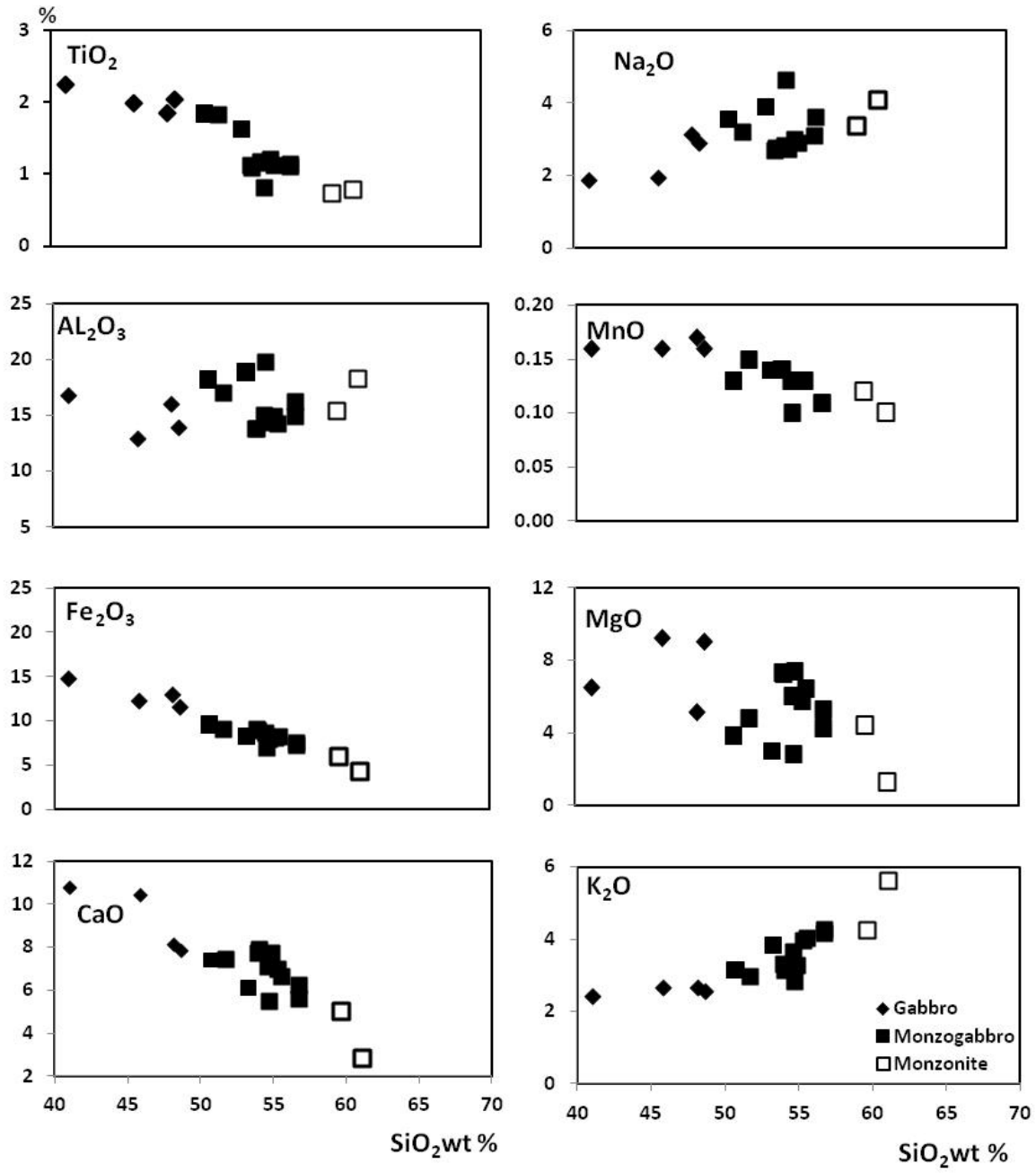

Fig.3: Variation diagrams of selected major elements plotted against SiO_2 for the Bayon plutonic rocks.

Table 2: Major, trace and rare earth elements from

	Gabbro				Monzogabbro												Monzonite	
Sample	BA6	F16	K3	K4	BA3	BA4	BA2	F14	F15	BA5	MBA1	F8	F12	B2	B5	B1	B10	MBA2
SiO_2 %	41.00	45.81	48.13	48.62	50.71	53.29	51.68	53.93	54.01	54.58	54.66	54.81	55.26	55.51	56.69	56.70	59.58	61.06
TiO_2	2.24	1.99	1.86	2.04	1.84	1.62	1.84	1.13	1.09	1.19	1.16	0.83	1.21	1.13	1.15	1.11	0.74	0.79
Al_2O_3	16.79	12.99	16.08	13.94	18.21	18.86	17.06	13.81	13.82	15.06	19.82	14.38	14.89	14.33	14.92	16.31	15.36	18.27
Fe_2O_3	14.80	12.36	13.08	11.63	9.61	8.24	9.11	9.09	9.00	8.65	7.00	8.05	8.12	8.20	7.62	7.35	5.99	4.37
MnO	0.16	0.16	0.17	0.16	0.13	0.14	0.15	0.14	0.14	0.13	0.10	0.13	0.13	0.13	0.11	0.11	0.12	0.10
MgO	6.48	9.23	5.13	9.02	3.83	2.97	4.78	7.32	7.25	6.02	2.84	7.38	5.74	6.46	5.26	4.26	4.38	1.28
CaO	10.85	10.46	8.17	7.89	7.39	6.11	7.48	7.76	7.93	7.15	5.52	7.75	7.00	6.67	6.27	5.67	5.08	2.89
Na_2O	1.88	1.94	3.16	2.91	3.55	3.90	3.20	2.70	2.76	2.85	4.64	2.74	2.99	2.92	3.10	3.63	3.37	4.10
K_2O	2.42	2.67	2.66	2.56	3.15	3.83	2.98	3.34	3.17	3.66	2.83	3.28	3.96	4.06	4.27	4.17	4.24	5.63
P_2O_5	1.34	1..37	1.15	1.01	0.88	0.63	0.81	0.72	0.73	0.73	0.49	0.73	0.71	0.71	0.63	0.62	0.46	0.22
LOI	1.34	0.29	0.32	0.07	0.11	0.12	0.23	0.10	0.07	-0.13	0.61	0.03	-0.01	0.00	-0.11	-0.04	0.13	0.32
Total	99.30	99.27	99.91	99.85	99.41	99.71	99.32	100.04	99.97	99.89	99.67	100.11	100.00	100.12	99.91	99.89	99.45	99.03
Alk	4.30	4.61	5.82	5.47	6.70	6.70	6.18	6.04	5.93	6.51	7.47	6.02	6.95	6.98	7.37	7.80	7.61	9.73
Ba (ppm)	3362	4283	3075	2601	4217	3713	3177	2064	1940	2560	1947	1546	2737	2390	2205	8102	2798	5875
Co	41	52	39	51	24	21	25	37	36	27	16	28	29	29	27	134	17	7
Cr	35	361	5	430	12	10	111	348	344	231	32	338	225	293	233	597	181	<2
Cu	28	87	33	35	18	9	40	48	45	36	28	18	34	43	34	178	24	6
Ga	30	22	26	23	27	25	23	20	19	20	30	92	20	19	21	22	20	22
Mo	Na	Bdl	1.00	Na	bdl.	Na	bdl.	1.00	1.00	Na	Na	Na	1.00	1.00	2.00	Na	Na	Na
Nb	6	9	10	13	14	11	12	9	9	9	14	8	10	12	14	9	14	10
Ni	16	89	5	122	11	15	46	77	75	76	23	91	50	82	52	36	93	11
Pb	Na	12	18	Na	19	Na	20	20	21	Na	Na	Na	21	25	25	Na	Na	Na
Rb	106	111	117	69	82	91	95	116	109	106	126	107	113	140	161	111	153	164
Sc	29	31	33	16	20	15	21	22	23	23	13	24	20	19	17	40	11	7
Sr	1636	1368	1295	1261	1728	1397	1535	1091	1081	1041	1425	984	1086	1010	948	979	1199	1125
V	365	394	404	220	244	171	229	252	241	192	118	150	202	189	179	123	112	65
Zn	144	148	149	127	104	122	104	98	98	98	99	92	92	93	92	415	92	84
Sr	1636	1368	1295	1261	1728	1397	1535	1091	1081	1041	1425	984	1086	1010	948	979	1199	1125
V	365	394	404	220	244	171	229	252	241	192	118	150	202	189	179	123	112	65
Zn	144	148	149	127	104	122	104	98	98	98	99	92	92	93	92	415	92	84
Zr	149	89	105	135	144	278	123	138	139	196	173	219	126	196	244	158	163	266
Li	Na	48.27	45.82	39.82	582.03	Na	18.43	19.44	18.32	Na	Na	Na	18.10	50.48	18.60	20.81	Na	Na

Table 2:(continued)

	Gabbro				Monzogabbro												Monzonite	
Sample	BA6	F16	K3	K4	BA3	BA4	BA2	F14	F15	BA5	MBA1	F8	F12	B2	B5	B1	B10	MBA2
Be	Na	1.31	1.79	1.14	1.56	Na	1.61	1.69	1.77	Na	Na	Na	1.64	2.09	2.39	2.16	Na	Na
Y	19.90	26.04	26.83	24.10	26.37	26.86	20.42	21.70	21.57	20.79	23.02	20.84	21.20	20.57	20.97	29.04	18.49	14.39
Sn	Na	2.01	2.74	1.65	2.72	Na	2.46	2.00	1.91	Na	Na	Na	1.60	2.28	2.37	2.23	Na	Na
Hf	Na	2.25	1.07	0.87	1.48	Na	1.22	2.04	2.66	Na	Na	Na	1.77	1.22	2.71	1.62	Na	Na
Ta	Na	0.51	0.73	0.72	1.20	Na	1.16	0.73	2.37	Na	Na	Na	0.86	0.96	1.09	1.03	Na	Na
Th	1.20	3.60	3.87	2.97	2.16	1.81	4.23	5.58	5.65	3.84	3.30	4.08	4.37	6.98	9.47	6.33	9.42	5.74
U	0.23	0.59	0.93	0.36	0.35	0.30	0.86	1.08	1.13	0.81	0.91	0.93	0.80	1.29	1.98	1.23	2.69	1.14
K	20090	22165	22082	21252	26150	31795	24739	27728	26316	30384	23494	27229	32875	33705	35448	34618	35199	46738
Ba/Rb	31.74	38.73	26.35	37.70	51.49	40.62	33.37	17.84	17.81	24.06	15.43	14.42	24.18	17.08	13.69	71.70	18.30	35.85
Ba/Sr	2.05	3.13	2.37	2.06	2.44	2.66	2.07	1.89	1.79	2.46	1.37	1.57	2.52	2.37	2.33	8.28	2.33	5.22
Rb/Sr	0.06	0.08	0.09	0.05	0.05	0.07	0.06	0.11	0.10	0.10	0.09	0.11	0.10	0.14	0.17	0.12	0.13	0.15
Rb/Ba	0.03	0.03	0.04	0.03	0.02	0.02	0.03	0.06	0.06	0.04	0.06	0.07	0.04	0.06	0.07	0.01	0.05	0.03
K/Rb	189.71	200.41	189.22	308.00	319.29	347.87	259.86	239.65	241.65	285.56	186.16	254.01	290.41	240.92	220.04	306.35	230.21	285.16
La (ppm)	29.10	42.09	53.33	53.18	51.72	48.60	41.19	38.90	39.54	38.72	61.42	38.36	39.76	44.40	44.50	46.09	50.05	45.31
Ce	59.09	97.44	119.03	119.30	123.47	106.27	91.23	86.84	88.38	76.03	96.31	69.53	86.55	96.52	95.77	96.56	99.24	62.98
Pr	8.63	12.81	15.08	14.86	16.30	13.71	11.39	10.76	10.97	9.47	11.67	9.60	10.59	11.71	11.44	11.60	10.52	8.71
Nd	47.08	58.17	65.19	61.96	70.79	56.97	48.60	45.82	46.18	39.77	43.05	44.79	44.31	47.97	46.03	47.38	34.85	40.49
Sm	9.82	12.13	12.55	11.52	13.11	13.42	9.47	9.12	9.13	9.10	9.24	8.86	8.85	9.23	8.95	9.16	8.88	8.86
Eu	3.02	3.31	3.32	3.21	4.13	4.23	3.24	2.40	2.41	2.69	3.12	2.30	2.70	2.58	2.43	2.64	2.88	4.83
Gd	8.04	10.82	11.12	10.15	11.00	10.58	8.24	8.24	8.24	7.91	9.06	7.91	7.86	8.15	7.83	8.37	7.65	5.77
Tb	0.99	1.20	1.26	1.13	1.23	1.32	0.94	0.96	0.97	0.93	1.10	0.98	0.89	0.91	0.90	0.97	0.88	0.67
Dy	4.61	5.70	5.83	5.32	5.69	6.19	4.38	4.65	4.62	4.45	5.26	4.68	4.25	4.31	4.31	4.73	4.12	3.13
Ho	0.76	0.99	1.03	0.92	0.98	1.04	0.78	0.83	0.83	0.75	0.88	0.79	0.77	0.76	0.76	0.89	0.69	0.53
Er	2.05	2.55	2.64	2.41	2.58	2.87	2.07	2.22	2.18	2.17	2.44	2.28	2.05	2.04	2.07	2.44	2.05	1.57
Tm	0.24	0.31	0.32	0.29	0.32	0.33	0.26	0.29	0.30	0.27	0.29	0.29	0.27	0.27	0.27	0.31	0.27	0.20
Yb	1.48	2.00	1.97	1.87	2.01	2.01	1.71	1.90	1.88	1.78	1.79	1.54	1.79	1.76	1.80	2.04	1.83	1.31
Lu	0.2	0.29	0.28	0.27	0.28	0.26	0.25	0.28	0.29	0.25	0.23	0.27	0.27	0.26	0.26	0.31	0.26	0.18

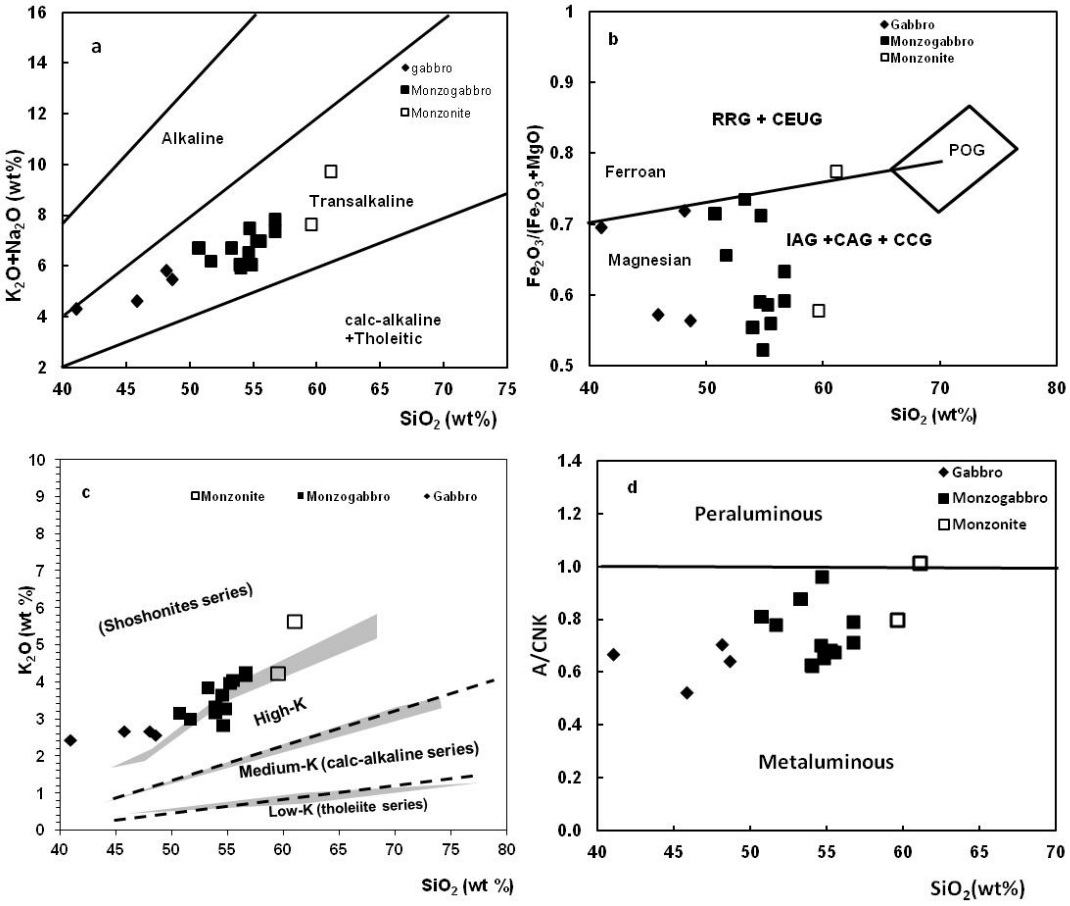

Fig. 4 a) The studied granitoids in the TAS diagram with fields after *Middlemost(1997)*; b) The composition range of the Bayon granitoids in the $FeO^{tot}/(FeO^{tot}+MgO)$ vs SiO_2 diagram. Fields are from Frost et al., (2001). The fields of RRG+CEUG (anorogenic granitoids); POG (Post-orogenic granitoids) and IAG+CAG+CCG (orogenic granitoids) after *Pearce et al., (1984)*. c) K_2O vs SiO_2 diagram illustrating the high-K calc-alkaline and shoshonitic affinities of the Bayon granitoids. The fields after *Le Maitre et al.,(1989) and Pecerillo et Taylor*(1976). d) Molar $Al_2O_3/(CaO+Na_2O+K_2O)$ vs SiO_2 diagram of the studied rocks (Chappell and White, 1992).

Trace and Rare Earth elements

Trace and Rare Earth element content of the representative studied rocks are show in Table 2. The gabbro has high abundance of Sr, Ba, V and Zr but possesses low concentrations of Rb, Sc, Y and Th. The monzogabbro has high concentration of Ba, Sr, Zr, V and Cr except for one sample (MBA1), which displays low chromium content. Monzogabbro has low concentration of Zn while B1 sample displays high content and moderate concentration of Rb and low concentration of Sc and Y. Ba, Cr, Zn content in B1 sample is high. Element distribution shows that gabbroic rocks have high contents ofLILE (Large ionic lithophile elements) such as Ba, Sr, except Rb(69-126ppm). They have low content of High Field Strength Elements(HFSE) as Nb (6-23ppm), Th(1.20-9.47ppm) and Pb (12-25ppm) except Zr (89-278ppm). Compatible elements in gabbroic rocks show a rather strong Cr concentration, which varies between111 and 597ppm, except for samples K3, BA3, BA4 and MBA1. The monzonite samples contain high concentration of Ba, Sr, Rb, Zr and Cr except in sample MBA2 (Cr< 2ppm).

In the chondrite normalized Rare Earth Elements (REE) diagram (Fig. 5a, 5b), all the Bayon gabbroic rocks exhibit Light Rare Earth Elements (LREE) enrichment with (La_N/Yb_N=14.10-20.37) and without Eu anomalies (Eu/Eu*=0.86 to 1.12). In the primitive mantle normalized trace element spiderdiagram (Fig. 6a, 6b), Bayon gabbroic rocks characterized by enrichment in large ion lithophile elements (LILE) such as Ba, Sr but depleted of Th, P, Ce, Nb and the high-field-strength elements (HFSE) such as Ta and Ti. Positive anomalies in Sr, K, Smand Ba were noted.

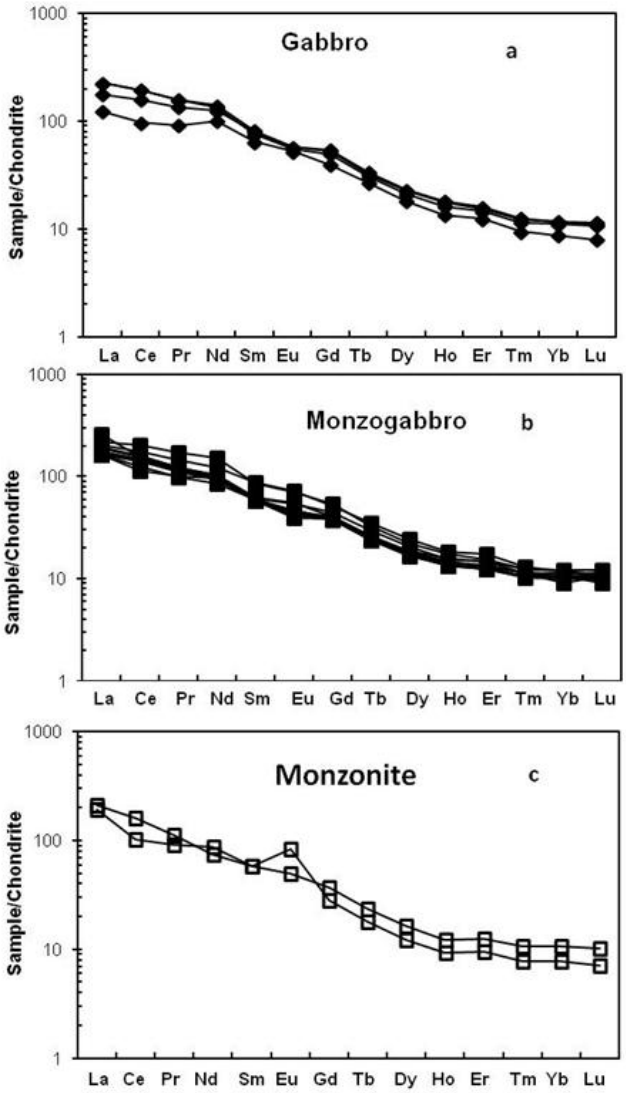

Fig. 5. Chondrite-normalised REE patterns for the Bayon plutonic rocks. Normalising values from *Sun and McDonough (1989).*

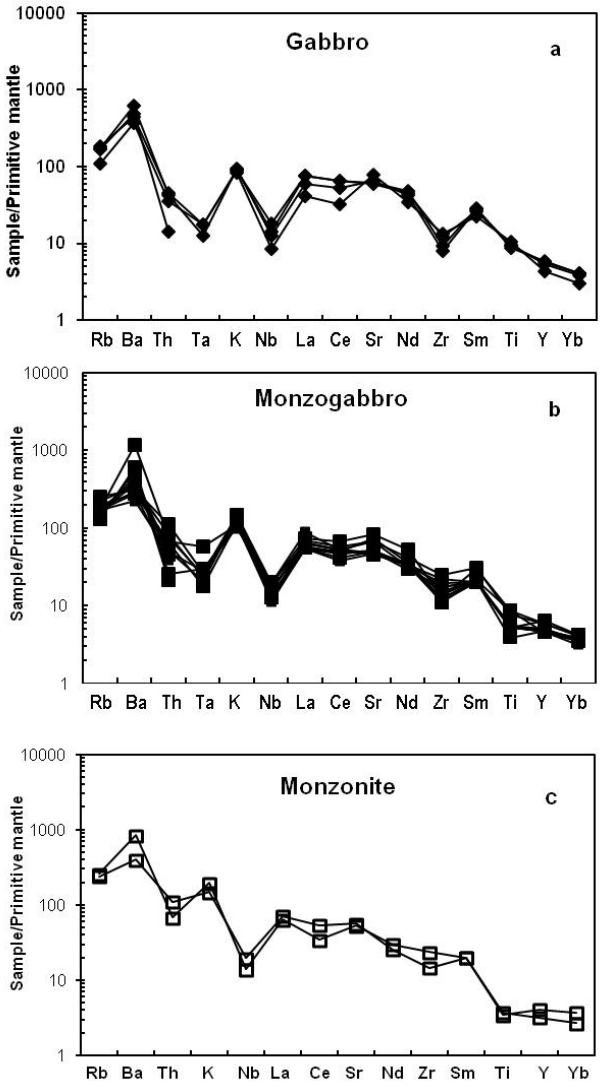

Fig. 6. Primitive mantle normalized trace element distributionfor the Bayon plutonic rocks. Normalising values fromSun and McDonough *(1989).*

Monzonitesamples are characterized by REE content ranging from 184.54 to 224.17ppm with LREE more enrichedcompared to HREE (Fig. 5c). This is expressed by La_N/Lu_N=20.63 -26.98 and La_N/Yb_N=19.62-24.81. The LREE and HREE showed slight fractionation with La_N/Sm_N=3.30-3.64 and Gd_N/Yb_N=3.46-3.64. The moderate positive Eu (Eu/Eu*=1.07-2.07) anomaly is dominant in all the monzonite samples (Fig. 6c). The patterns revealed the depletion in Nb, Th, Ce, P and Ti and positive anomaly at Ba, and K.These small to negligible Eu anomalies and the high Sr contents exclude important fractional crystallization of feldspar in the Bayon plutonic rocks petrogenetic evolution.

Sm-Nd isotopes

The Sm-Nd data for the Bayon plutonic rocks are presented in Table 3. In samples BA5 and mineral fractions, the Sm/Nd-wr-Cpx-Pl isochron yielded 580 ± 13 Ma with the initial $^{143}Nd/^{144}Nd$ ratio of 0.511577 ± 0.000011 and a (MSWD) = 0.107 (Table 3, Fig.7a). From sample F8, the wr and handpicked minerals (two clinopyroxenes fractions Cpx1 and Cpx2; plagioclase and apatite) define an isochron corresponding to an age of 577 ± 49 Ma and the initial $^{143}Nd/^{144}Nd$ ratio of 0.511572 ± 0.000040 and a MSWD =0.107 (Table 3, Fig. 7b). wr sample BA4, pyroxene and plagioclase isochron age yielded 553 ± 32 Ma with an initial

$^{143}Nd/^{144}Nd$ ratio of 0.511498 ± 0.000027 and MSWD = 3.6 (Table 3, Fig. 7c). The wr, clinopyroxene and plagioclase fractions from the MBA2 sample give an isochron age of 547 ± 26 Ma, an initial $^{143}Nd/^{144}Nd$ ratio of 0.511470 ± 0.000019 and a MSWD = 5.1 (Table 3, Fig. 7d). The slight deviation of the whole rock from the mineral isochron may results in a large age error and could probably be related to random Nd isotope perturbation via high temperature hydrothermal fluids related to the crystallization of hydrous phases such as hornblende and phlogopite. The single sample F14 whole rock composition analysed using DM parameters of *Michard et al. (1985)*gives a TDM model age at ca. 1600 Ma for monzogabbro. Since they have similar Nd isotopic values, it is possible that they originate from the same magmatic episode. No Sm-Nd isochron can be obtained because of the very small variations in the isotopic values. The negative initial εNd values that range between -6 and -9, suggest the dominanceofenriched crustal component of the protolith.

Table 3: Sm/Nd isotope data of analyzed samples

Rock types and samples	Sm(ppm)	Nd(ppm)	$^{147}Sm/^{144}Nd$	$^{143}Nd/^{144}Nd$	±2σ	$^{143}Nd/^{144}Nd_{init}$	ε Nd(0)	ε Nd(t)	T_{DM}(Ga)	Age (Ma)
Monzogabbro										
BA4(Wr)	13.32	69.07	0.116500	0.511918	0.000002	0.511498	-14.0	-8.3	1.7236569	**553±32 Ma MSWD=3.6 n=3**
BA4(Cpx)	26.77	111.60	0.145000	0.512025	0.000002	0.511498	-11.9	-8.3	2.147367	
BA4(Pl)	3.096	19.15	0.097700	0.511862	0.000012	0.511498	-15.1	-8.3	1.5324185	
Monzogabbro										
BA5(Wr)	9.12	47.25	0.116630	0.512019	0.000003	0.511577	-12.0	-6.1	1.5807839	
BA5(Cpx 1)	20.11	78.32	0.155230	0.512167	0.000002	0.511577	-9.1	-6.1	2.1534218	**580±13Ma MSWD=0.107 n=4**
BA5(Cpx 2)	19.87	76.97	0.156050	0.512170	0.000001	0.511577	-9.1	-6.1	2.1731495	
BA5(Pl)	0.65	5.67	0.068780	0.511839	0.000006	0.511577	-15.5	-6.1	1.2671156	
F8(Wr)	9.53	48.73	0.118150	0.512022	0.000002	0.511572	-12.0	-6.3	1.5994291	
F8(Cpx1)	17.49	70.24	0.150510	0.512146	0.000005	0.511572	-9.6	-6.3	2.0564991	
F8(Cpx2)	17.46	69.81	0.151190	0.512144	0.000004	0.511572	-9.7	-6.3	2.0888955	**577±49Ma MSWD=2.9 n=5**
F8(Pl)	1.80	11.51	0.094580	0.511932	0.000004	0.511572	-13.7	-6.3	1.4118726	
F8(Ap)	295.10	1575	0.113240	0.511995	0.000002	0.511572	-12.5	-6.3	1.5651591	
F14(Wr)	9.66	49.05	0.119040	0.512026	0.000002	0.511576	-11.9	-6.1	1.607304	
Monzonite										
MBA2(wr)	6.43	37.82	0.102800	0.511832	0.000002	0.51147	-15.7	-9.1	1.6358566	**547±26Ma MSWD=2.8 n=2**
MBA2(Cpx)	29.78	146.2	0.123150	0.511912	0.000002	0.51147	-14.1	-9	1.8480889	
MBA2(Pl)	0.86	6.80	0.076570	0.511745	0.000006	0.51147	-17.4	-9	1.432635	

Sm/Nd isotope data of analyzed samples. Initial values are recalculated to553-525 Ma for gabbro; 572-580 Ma for monzogabbro and 547 Ma for monzonite.εNd (0) = $^{143}Nd/^{144}Nd)_s/(^{143}Nd/^{144}Nd)_{CHUR}$-1)*10000. εNd (0) is the value of εNd at the present time. $(^{143}Nd/^{144}Nd)_{CHUR}$=0.512638 and $(^{147}Sm/^{144}Nd)_{CHUR}$=0.1967 (Faure, 1986).$T_{Dm}$ were calculated based on present day DM values of $(^{143}Nd/^{144}Nd)_{DM}$=0.513114and$(^{147}Sm/^{144}Nd)_{DM}$=0.222. *(Michard et al., 1985).*I_{CHUR}(580 Ma) =0.511890

Table 4: Rb/Sr isotope data of analyzed samples.

	Rb(ppm)	Sr(ppm)	$^{87}Rb/^{86}Sr$	$^{87}Sr/^{86}Sr$	±2Sm	$^{87}Rb/^{86}Sri$	εSr(0)
Gabbro							
K4(Wr)	79.18	1339	0.1712	0.708806	0.000004	0.70746	61.1
Monzogabbro BA4(Wr)	86.24	1469	0.1699	0.708816	0.000004	0.70746	61.3
BA4(Bt)	446.9	20.78	65.41	1.227199	0.000024		
BA5(Wr)	99.07	1101	0.2605	0.709211	0.000004	0.707195	66.9
BA5(Bt)	618.7	17.51	110.9	1.565342	0.000012		
F8(Wr)	99.09	1033	0.2777	0.70934	0.00005	0.707201	68.7
F8(Bt)	598.3	16.45	114.3	1.587702	0.000027		
F14(Wr)	104.2	1037	0.2908	0.709449	0.000005	0.7072	70.2
Monzonite							
MBA2(Wr)	162	1265	0.3702	0.710767	0.000004	0.708257	89.0

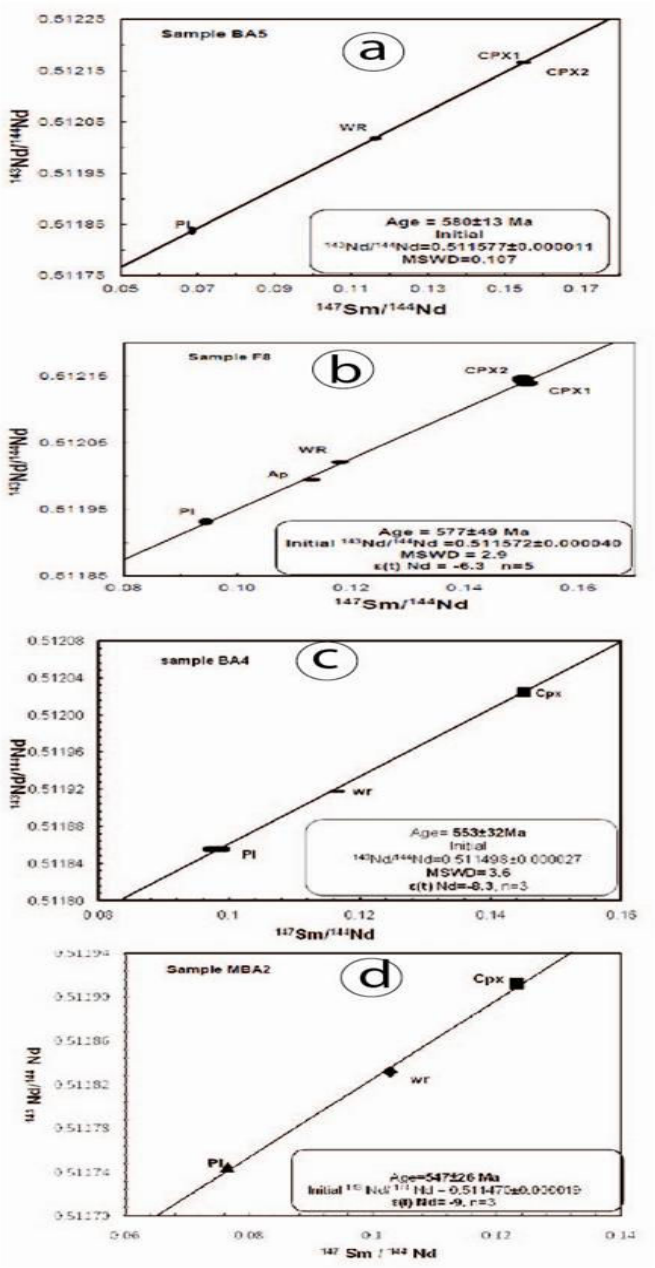

Fig. 7. The Bayon plutonic complex Sm/Nd-WR-Px-Pl isochron ages.

DISCUSSION

Geochemical evolution

Geochemical studies of Bayon plutonic rocks show two groups: gabbroic rocks (gabbro l.s., and monzogabbro) and monzonite. All these rocks have the same mineral assemblage; however, little quartz occurs in the monzonite and in some Monzogabbro samples. Major and trace elements variations show a continuity between gabbroic rocks and monzonite. These rocks showed the least scatter of data(Fig. 3)with negative correlations between SiO_2 and MgO, Fe_2O_3, CaO, P_2O_5, MnO, TiO_2. Alternatively, K_2O, Al_2O_3 and Na_2O correlated positively with SiO_2. The important feature in the data is the presence of little gap at 56.70 – 59.58 % SiO_2 separating the gabbroic rocks from monzonite in two distinct groups. The increase in Na_2O content and the decrease in MgO, Fe_2O_3, CaO, TiO_2 and P_2O_5 at 45.52 wt% SiO_2 showed that fractionation of mafic mineral took place in the early stages of crystallization. In gabbro, the corresponding mineral was pyroxene. The higher value of P_2O_5 in some gabbros samples could be linked to the presence of the apatite phase. The high levels of total alkalis and aluminium in the monzogabbro

and monzonite can be explained by the presence of alkali-feldspar. Higher TiO_2 and Fe_2O_3 are due to iron oxide, which is represented by ilmenite and magnetite. The abundance of TiO_2 decreased with increase in SiO_2, which could imply crystallization of titaniferous magnetite indicating relatively high fO_2 in the melt. According to the total alkali content (∑alkali = 4.30 – 9.73wt %), the (Na_2O+K_2O) vs SiO_2 diagram (Fig. 5a) (TAS diagram with fields after *Middlemost, 1997*), the studied rocks exhibit a trans-alkaline character and showa positive correlation between SiO_2 content and the alkalis. It is noted also that the Bayon plutonic rocks plot within the high-K to shoshonitic fields. The similarities of REE and multi-elements patterns for gabbroic rocks and monzonite associated with some trends in Harker diagrams suggest that those lithologies are cogenetic and that fractional crystallization could have played an important role in the generation of the magma. The homogeneity of geochemistry and isotopic significance of mafic and intermediate Bayon rocks show that they have close genetic relationships. The Bayon plutonic rocks which are enriched in LILE including K, Rb, Sr and Ba relative to the HFSE especially Zr, Nb and Y can be compared to the shoshonitic association which main characteristic are: high total alkalis ($Na_2O+K_2O>3$), low TiO_2 (<1.3wt%), high contents of LILE(Ba, Sr, Rb), low Nb and no Fe enrichment*(Morrison, 1980)*.The presence of coupled Ta, Nb and Ti negative anomalies in spider diagram could be an indication of the contribution of subduction related components. The little scatter of data in major, trace and isotopic composition diagrams could be explained by the contamination of primitive melts by crustal components(*Huppert and Sparks, 1985*).

Source and tectonic setting

A question always emerging from the study of rocks is whether magma source were located in the sub-continental lithospheric mantle (SCLM) or in the asthenosphere. Determinationofthe source of the magma composition is highly difficultbecause there are several mantle components (DMM, HIMU, EM1, EM2).Some authors*(Coish and Sinton, 1992)*have used La/Ta and La/Nb ratios to distinguish lithospheric (La/Ta > 22; La/Nb > 1.5) fromasthenospheric sources which would be characterized by La/Ta < 22; La/Nb < 1.5. The Bayon rocks are characterized by ratios (La/Ta = 36-80; La/Nb=3-5). On the other hand, the nature of the igneous source can be constrained using the geochemical and isotopic signatures of plutonic rocks. The Nb/Zr vs Nb/Ba diagram of*Hopper and Hawkesworth, (1993)*(Fig. 8)shows that the gabbroic rocks (gabbros s.l. and monzogabbro) and monzonite originated from partial melting of an enriched subcontinental lithospheric mantle(SCLM). The studied samples are also most radiogenic and are enriched in large ion lithophile elements; they have high $^{87}Sr/^{86}Sr$ and low $^{143}Nd/^{144}Nd$ and; the Nd T_{DM} model age ranges around 1.6 to 1.7 Ga. According to *Zindler and Hart, (1986),* the sample which has these signatures (high $^{87}Sr/^{86}Sr$ and low $^{143}Nd/^{144}Nd$), originates from enriched mantle (EMII).The spider diagrams of the Bayon plutonic rocks are almost similar. The gabbroic rocks and monzonite are high – K calc- alkaline to shoshonitic I-type granite; however High-K calc-alkalinerocks often occur in the continental arc setting or the late collision setting; sometimes they evolve to shoshonitic composition or peralkaline in the final stage of the orogeny*(*Liegeois et al., 1998).

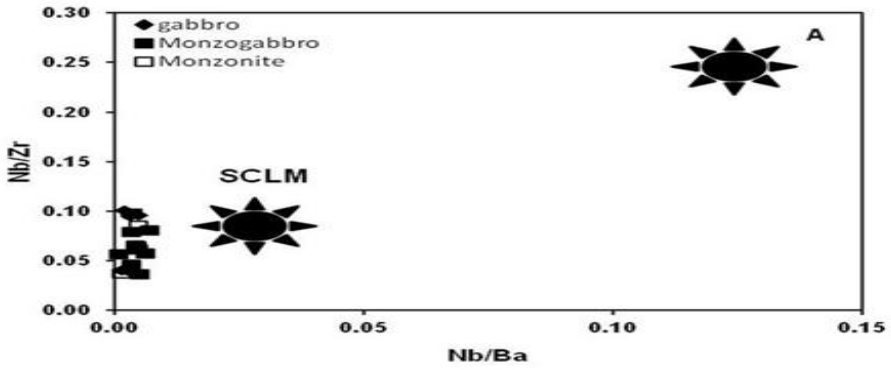

Fig.8. Nb/Zr vs Nb/Ba diagram after showing position of Bayon plutonicrocks. *Hopper and Hawkesworth (1993).*SCLM **=** subcontinental lithospheric mantle, A = asthenosphere.

Trans-alkaline characters as well as high-K to shoshonitic enrichments suggest that Neoproterozoic magmatism initially with calc-alkaline characters evolved towards alkalinity at the end of the Precambrian; this evolution predates alkaline affinities of the magmatism of the region during the Tertiary after a gap (absence of magmatic activity) running from the Cambrian to the Tertiary.Potassic contents of rocks in the Bayon plutonic complex are compatible with these age data since the incompatible element composition of the gabbroic rocks shows close similarities with those of the magmatic arc granitoids, e.g. the enrichment in LILE and LREE with depletion at Nb and Ti *(Pearce et al., 1984)*.All the Bayon plutonic rocks areenriched in Ba and Sr. This enrichment is probably inherited from such an enriched mantle *(Chen et al., 2002)*.Initial $^{87}Sr/^{86}Sr$ ratio is slightly different but generally high in the different groups of the rocks, meaning that they are similar in the source. Relatively high $^{87}Sr/^{86}Sr$ ratio suggests that the Bayon plutonic rocks were derived from or were contaminated

with crustal material. When compared to the mantle values, the samples are enriched in large ion lithophile elements; have high $^{87}Sr/^{86}Sr$ (Table 4) and low $^{143}Nd/^{144}Nd$ with the Nd T_{DM} model age ranging from 1.6 to 1.7 Ga.In the Sr – Nd correlation diagram (Fig. 9b), it is evident that all the analysed rocks plot in the right lower quadrant which reflects the enriched sources, suggesting that the magma from these rocks originated from the same source as mentioned above.The T_{DM} ages of the studied rocks range from 1.6 to 1.7 Ga with negative εNd (600) between -6.1 to -9.2. This result agrees with the remnants of Mesoproterozoic crust in this area of CAFB. The Nd and Sr isotopic from Bayon plutonic rocks*(Ngo Belnoun, 2008)* indicate the slow differential cooling age of the intrusive rocks.The tectonic discrimination diagrams for granitoids Rb vs Y+Nb (Peace, 1996) shows that all the samples clearly plot in the field of post collisional granite (Fig. 9a). In the Zr vs $(Nb/Zr)_N$ diagram (Fig. 9b) of*Thiéblemont and Tegyey* (1994), all the studied samples plot again in the field of collision zone rocks. All these characteristics and high-K calc-alkaline affinity are consistent with an orogenic collision setting (Liégeois et al.,1998).The diagram of Frost et al., 2001(Fig. 4b) clearly indicates that the rocks are magnesian and the plot in field ofthe diagram ofPearce et al., (1984), shows that the studied rocks are situated in the field of orogenic granitoids.

Implications for regional geodynamics

The Bayon plutonic complex compared to some massifs in West Cameroon shows that it is less potassic than the other studied complexes (Fig. 10).Comparative studies of incompatible trace elements versus primitive mantle of Sun and *McDonough* (1989)of data from the Bayon plutonic complex and some massifs of West Cameroon (Bafoussam, Ngondo) show similarities in terms of negative anomalies in Nb, Ce, Ti (Fig. 11)which represent signatures of subductional and collisional events. Such evidenceis also found when the Fomopéa granitoids are compared to the Bayon intrusive rocks. The Bayon plutonic rocks that have high content of alkali, Ba and Sr are also similar to the calc-alkaline to transitional granitoids of the Solidao type *(Guimarães et al., 1998; Guimarães and da Silva Filho, 2000).*

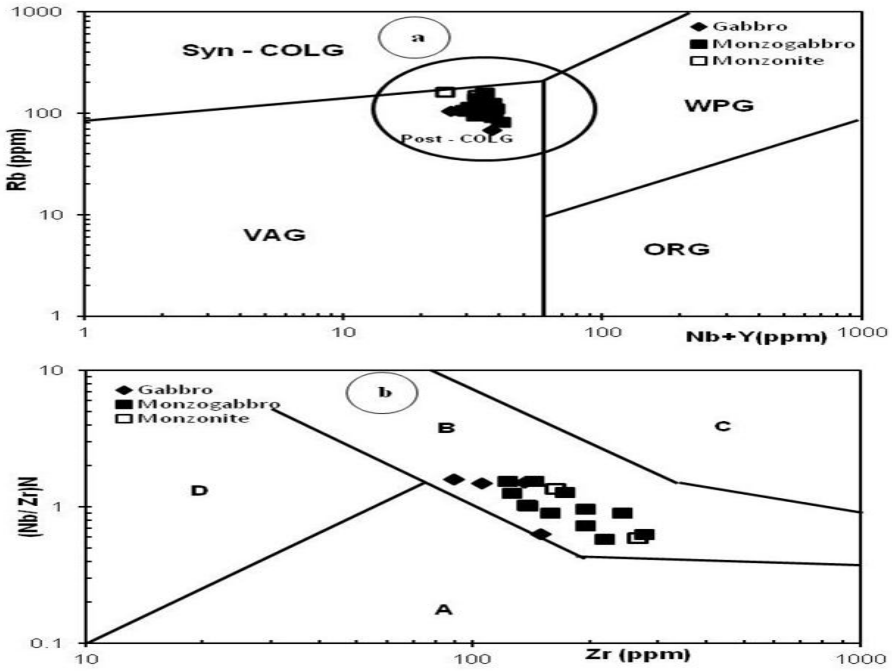

Fig. 9. Tectonic diagrams for Bayon plutonic rocks. a) Rb vs (Y+Nb) with discrimination fields after *Pearce(1996)*. WPG=within plate granites; ORG= oceanic ridge granites; VAG= volcanic arc granites; Syn-COLG= syn-collisional granites; Post-COLG= post –collisional granites. b) Zr vs $(Nb/Zr)_N$ diagram of *Thiéblemont and Tegyey (1994)* for Bayon granitoids. A= subduction-zone magmagtic rocks; B= collision zone rocks; C= alkaline intraplate zone rocks. Normalization to primitive mantle value from *Sun and McDonough* (1989).

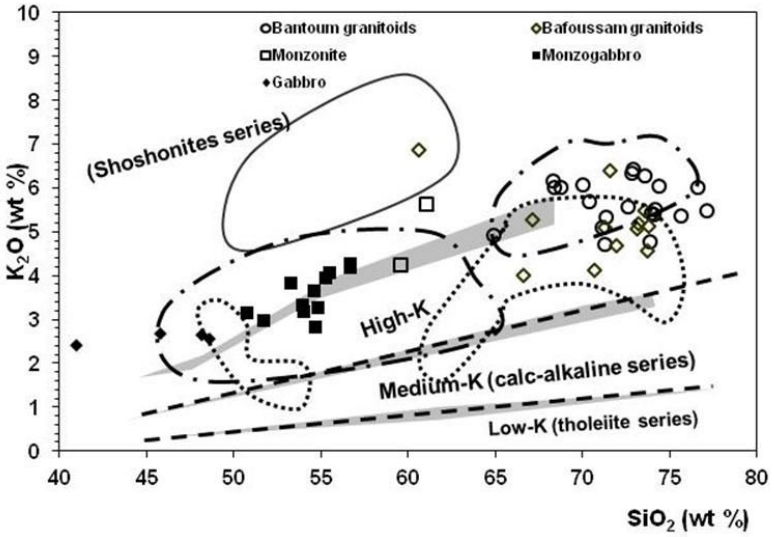

Fig.10. Classification of some study plutonic rocks in the K_2O – SiO_2 diagram. The different fields are after Le *Maitre et al.,*(1989) *and Peccerillo and Taylor* (1976). Dash line = Ngondo plutonic rocks; Black circle = Bangangte syenite; dotted line = Fomopea plutonic rocks. This diagram shows that Bayon plutonic complex has almost the same geochemical affinity.

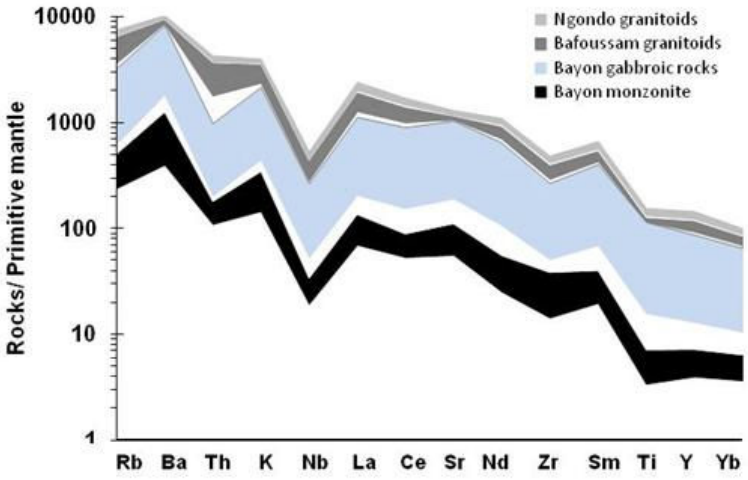

Fig.11. Multi-element primitive mantle plot (normalizing values from Sunand *McDonough* (1989)to compare Bayon plutonic rocks and some West Cameroon massifs(Ngondo and Bafousssam).

CONCLUSION

The Bayon plutonic complex is composed of gabbroic (gabbro s.l. and monzogabbro) and monzonite rocks.The major minerals areplagioclase, augite, diopside, pigeonite, clinoenstatite, and biotite. Orthoclase is found in monzogabbro and monzonite, whilst quartz is found only in the monzonite samples. Accessory minerals common in the gabbroic and monzonitic rocks are ilmenite, magnetite, apatite, titanite and zircon. Geochemicaldata indicate that the Bayon plutonic rocks are transalkaline, metaluminous, magnesian, I-type and have high-K to shoshonitic affinities.The primitive mantle normalized trace element

patterns display Nb, Ti, Ta, negative anomalies.Chondrite-normalized rare earth elements patterns indicate the enrichment ofLREE and flat patterns of HREE. εNd (600) vs $^{87Sr}/^{86}Sr$ at 600 Ma diagram suggesting that the studied rocks were derived from enriched mantle with a little continental crust contamination. In all the discrimination diagrams, all the rocks studied fall within the collision zone. Geochemical variation of the Bayon plutonic rocks suggests that fractional cystallisation and crustal contamination may have taken place during the evolution of the magma. The Bayon plutonic rocks were generated by differentiation of mafic magma derived from enriched subcontinental lithospheric mantle. The Sr-Nd isotopic composition indicates that the plutonic rocks have been produced by partial melting of a subcontinental mantle supported by their initial $^{87}Sr/^{86}Sr$(600Ma).
The Bayon plutonic rocks were emplaced in a subduction to collison tectonic environment. All isotopic ages from this study are almost identical; they are cooling ages and date most probably uplift linked to wrench tectonic event at ca 560Ma.

ACKNOWLEDGMENTS

This study was realized thanks to an Austrian Exchange Service (OeAD) scholarship to the first author. The XRF, ICP-MS and isotopic analyses were processed with the help of Peter Nagl, W. Körner, and M. Horschineg. Electron microprobe was possible with assistance of Franz Kiraly. Dr Alambert Nganwa and Pr Kamgang Pierrecritically reviewed the manuscript.

REFERENCES

Abdelsalam, M.G., Liegeois, J.P and Stern, R.J., 2002. Sahara Metacraton. Journal African Earth Sciences 34, 119-136.

Casting, C., Feybesse, J. L., Thieblemont, D., Triboulet, C and Chevremont, P., 1994. Palaeogeographical reconstructions of the Pan-African/Brasiliano Orogen; closure of an oceanic domain or intracontinental convergence between major blocks? Precambrian Research 69, 327-344.

Chapell, B.W and White, A.J.R., 1992.- I and S-type granites in the Lachlan fold belt. Trans.R.Soc. Edinburg, 83, 1-12.

Chen, B., Jahn, B. M and Wei C., 2002. Petrogenesis of mesozoic granitoids in the Dabie UHP complex, central China trace element and Nd – Sr isotope evidence. Lithos 60, 67 – 88.

Coish, R.A and Sinton, C.W., 1992. Geochemistry of mafic dikes in the Adirondacmountains: implications for the constitution of Late Precambrian mantle.Contributions to Mineralogy and Petrology 110, 500–514.

Djouka-Fonkwe M.L., Schulz, B., Schlussler, U., Tchouankoue, J.-P., Nzolang, C.,2008. Geochemistry of the Bafoussam Pan-African I- and S-type granitoids in western Cameroon.Journal of African Earth Sciences 50,148-167.

Dumort, J. C., 1968. Carte géologique de reconnaissance à l'échelle du 1/500000^{ième}, République Fédérale du Cameroun, Notice explicative sur la feuille Douala – Ouest, Direction des Mines et de la Géologie du Cameroun.

Feybesse, J. L., Johan, V., Triboulet, C., Guerrott, C., Mayayo-Mikolo, F., Bouchot, V and Eko NSdong, J.,1998. The West Central African Belt: a model of 2.5-2.0 Ga accretion and two phase orogenic evolution. Precambrian Research 87, 161-216.

Frost, B.R., Barnes,C.G., Collins, W.J., Arculus, R.J., Ellis, D.J., Frost, C.D., 2001.A geochemical classification for granitic rocks.Journal of petrology 42, 2033-2048.

Guimarães, I.P., da Silva Filho, F.A., Almeida, C.N., Araùjo, M:M:J:, Melee, S.C and Sales, A., 1998.The braziliano granitoidsfro the PajeuParaiba Belt and Texeira High: Sm-Nd isotope geochemistry and U/Pb in zircon ages. XL Congresso Brasileiro de Geologia (Belo Horizonte, Mg), Abstracts, p.48.

Guimarães, I.P and da Silva Filho, F.A.,2000. Evidence of multiple sources involved in the genesis of the neoproterozoic itapetim granitic complex, NE Brazil,

Hopper, P.B and Hawkesworth, C. J., 1993.Isotopic and geochemical constraints on the origin and evolution of the Columbia River basalts.Journal of Petrology 34, 1203 – 1246.

Huppert,H.E and Sparks, R. S. J., 1985. Cooling and contamination of mafic and ultramafic magmas during ascent through continental crust.Earth and lanetary Sciences Letters 74, 371-386.

Kwekam, M., Liégois, J.P., Njonfang, E., Affaton, P., Hartmann, G and Tchoua, F., 2010. Nature, origin and signification of the Fomopéa Pan-African high-K calc-alkaline plutonic complex in the Central African fold beld(Cameroon). Journal African Earth Sciences 57, 79-95.

Lassere, M. et Soba, D., 1979. Migmatisation d'âge panafricain au sein des formations camerounaises appartenant á la zone mobile de l'Afrique centrale. Comptes Rendus Académie Sciences Paris. Somm. Géol. Fr., pp. 64 – 68.

Le Maitre, R.W., Bateman, P., Dudek, A., Keller, J., Lameyre Le Bas M.J., Sabine, P.A., Schmid, R., Sorensen, H.,Streckeisen, A., Woolley,A. R and

zanettin, B.,1989. A classification of igneous rocks and glossary of terms: Recommendations of the International Union of geological Sciences, subcommission of the Systematics of igneous rocks. Black-well, oxford, 193pp.

Liégeois, J. P., Bertrand, J. M and Black, R., 1987.The subduction and collision – related Pan- African composite batholith of the Adrar des Iforas (Mali): a review. Geol. J. 22, 185-211.

Liégeois, J. P., Navez, J., Hertogen, J and Black, R., 1998. Contrasting origin of Post-collisional high-K calc-alkaline and shoshonitic versus alkaline and peralkaline granitoids: the use of sliding normalization. Lithos 45, 1 – 28.

Lindsley, D.H., 1983.Pyroxene thermometry. Am.Min.68, pp.477-493.

Ludwig, K.R., 2003. User's manual for Isoplot 3.00. A geochronological Toolkit for Microsoft Excel. Berkeley Geochronology Center, Special Publication No. 4a, Berkeley, California.

Lugmair, G.W and Marti, K., 1978. Lunar initial $^{143}Nd/^{144}Nd$: differential evolution of the lunar crust and mantle. Earth planet.Sci.lett.39, 3349-3357.

Mc Donough W.F., Sun, S.-S., Ringwood, A.E., Jagoutz, E and Hofmann, A.W., 1992. K, Rb and Cs in the Earth and Moon and the evolution of the Earth's mantle. Geochimica Cosmochimica Acta56, 1001–1012

Middlemost, E.A.K., 1997. Magma, Rocks and Planetary Development. Longman, Halow.

Morrison, G., 1980. Characteristics and tectonic setting oft he shoshonitic rock association. Lithos 13, 97-108.

Meschede, M., 1986. A method of discriminating between different types of mid-ocean ridge basalts and continental tholeiites with the Nb-Zr-Y diagram. Chemical geology 56, 207-218

Michard, P., Gurriet, P., Soudant, N and Albarède, F., 1985.Nd isotopes in french phanerozoic shales: external vs.internal aspects of crustal evolution. Geochimica Cosmochimica Acta 49, 601-610.

Mvondo, H., Owona, S., Mvondo, J and Essono, J., 2007. Tectonic evolution of the Yaounde segment of the Neoproterozoic Orogenic Belt in south Cameroon(Central Africa). Can. J. Earth Sci. 44, 443–444

Nédélec, A., Macaudière, J., Nzenti, J.P and barbey, P., 1986.Evolution structurale et métamorphique des schistes de Mbalmayo (Cameroun). Implication sur la structure de la zone Panafricaine d'Afrique Centrale au contact du craton du Congo. Comptes Rendus Académie des Sciences Paris 303, 75 – 80.

Ngako, V., Affaton, P., Nnangue, J. M and Njanko, T., 2003. Pan-African tectonic evolution in central and southern Cameroon; transpression and transtension during sinistral shear movements. Journal of African Earth Sciences 36, 207-214.

Ngnotue, T., Nzenti, J. P., Barbey, P. et Tchoua, F. M. 2000.The Ntui – Betamba high grade gneisses: a northward extension of the pan –African Yaounde gneisses in Cameroon. Journal of African Earth Sciences 31, 369 – 381.

Ngo Belnoun, R.N., 2008. Petrology, Mineralogy, Geochemistry and Geochronology of Kekem Mafic Complex, Western Cameroon PhD thesis, University of Vienna, Austria, 189p.

Nguiessi, T.C., Nzenti, J. P., Nkonguin Nsifa, E., Tempier, R. et Tchoua, F. M., 1997. Les granitoïdes calco – alcalins, syn – cisaillement de Bandja dans la chaîne Panafricaine Nord – Equatoriale. Comptes Rendus Académie des Sciences Paris 325, 95 – 101.

Njanko, T., 1999. Les granitoïdes calco–alcalins, syn–cisaillement de la région de Tibati (domaine central de la chaîne Panafricaine): leur signification géodynamique par rapport à la tectonique panafricaine. Thèse Doct. 3^{e} cycle, Univ. Yaoundel. 158p + Ann.

Njiekak, G., Dörr, W., Tchouankoué, J.-P. and Zulauf, G., 2008. U-Pb zircon and microfabrics data of(meta) granitoids of western Cameroun: Constraints on the timing of pluton emplacement and deformation in the Pan-African belt of central Africa**.** Lithos, Vol. 102, 3-4, (460-477).

Njonfang,E., Ngako, V., Moreau, C., Affaton, P and Diot, H., 2008. Restraining bends in high temperature shear zone: «The Central Cameroon Shear Zone » , Central Africa. Journal African Earth Sciences 52, 9-20.

Nzenti, J. P., Barbey, P., Bertrand, J. M. L. et Macaudiere, J., 1994.La chaîne Panafricaine au Cameroun: cherchons suture et modèle! In S. G. F edit. 15^{e} reunion des sciences de la terre, Nancy, France, p. 99.

Nzenti, J. P., Njanko, T., Njiosseu, E.L.T. et Tchoua, F. M., 1998.Les domaines granulitiques de la chaîne Panafricaine Nord – Equatoriale au Cameroun. In Géologie et environnements au Cameroun, Vicat et bilong eds, collect. Geocam I, pp. 255 – 264.

Nzolang, C., Kagami, H., Nzenti, J.P and Holtz, F., 2003. Geochemistry and preliminary Sr-Nd isotopic data on the neoproterozoic granitoïds from the Bantoum area, west Cameroon: evidence for a derivation from a paleoproterozoic to archean crust. Polar Geoscience16, 196-226.

Oliveira, E.P., Toteu, S.F., Araùjo, M.N.C., Carvalho, M.J., Nacimento, R.S., Buen, J.F., McNaughton, N., Basilici, G., 2006. Geologic correlation between the Neoproterozoic Sergipano belt (NE Brazil) and the Yaoundé schist belt (Cameroon, Africa). Journal African Earth Sciences 44, 470-478.

Owona, S., Schulz, B., Ratschbacher, L., Mvondo Ondoa, J., Ekodeck, G. E., Tchoua, F. M. and Affaton, P., 2011b. Pan-African metamorphic evolution in the southern Yaounde Group (Oubanguide Complex, Cameroon) as revealed by EMP-monazite dating and thermobarometry of garnet metapelites. Journal of African Earth Sciences 59, 125-139.

Owona, S., Tichomirowa, M., Ratschbacher, L., Mvondo Ondoa, J., Youmen, D., Pfänder, J., Tchoua, M.F., Affaton, P and Ekodeck, G.E., 2012. New igneous zircon Pb/Pb and metamorphic Rb/Sr ages in the Yaounde Group: implications for the Central African fold belt evolution close to the Congo Craton. Int. J. Earth. Sci. (Geol. Rundsch.), 101:1689–1703.

Pearce, J.A., Harris, N.B.W and Tindle, A.G., 1984. Trace element discrimination diagrams for the tectonic Journal of Petrology 25, 956–983.

Pecerillo,A.,Taylor,S.R.,1976. Geochemistry of Eocene calc-alkaline volcanic rocks from the Kastamonu area, northern Turkey. Contributions Mineralogy Petrology 58, 63-81.

Penaye, J., Toteu, S.F., Van Schmus, W.R., Tchakounté, J., Ganwa, A., Minyem, D and Nsifa, E.N., 2004. The 2.1-Ga West Central African Belt in Cameroon: extension and evolution, Journal of African Earth Sciences 39, 159-164.

Steiger, R.H and jaeger, E., 1977.Subcommission on geochronology**:** convention on the use of decay constants in geo- and cosmochronology, Earth planet.Sci. lett.36 (1977) 35

Sun, S.S and Mc Donough, W.F., 1989. Chemical and isotopic systematics of oceanic basalts: implications for mantle composition and process. In: Saunders A.D. and Norry M.J. (eds), magmatism in ocean basins. Journal of the Geological Society of London 42, 313-345.

Tagne, K. G., Mercier, E., Rossy, M. and Nsifa, N. E., 1999.Synkinematic emplacement of Pan-African Ngondo igneous complex (West- Cameroon, Central Africa). Journal of African Earth Sciences 28, 675-691.

Tagne, K. G., 2003. Petrogenesis of the Neoproterozoic Ngondo plutonic complex (Cameroon, West central Africa): a case of late-collision ferro-potassique magmatism.Journal of African Earth Sciences 36, 149-171.

Tchaptchet Tchato, D., Schulz, B and Nzenti, J.P., 2009. Electron microprobe dating and thermobarometry of Neoproterozoic metamorphic events in the Kekem area, Central African fold belt of Cameroon. N. Jb. Miner. Abh. 186/1, 95-109.

Tchouankoue, J.P., 1992.La syénite de Bangangté: un complexe panafricain à caractères intermediaires. Pétrologie-Géochimie. Thèse Doct. 3^{e} cycle Univ. Yaounde. 160p + ann.

Tetsopgang, S., 2003.Petrology, Geochemistry and geochronology of Pan-African granitoids in the Nkambé area. Northwestern Cameroon, Africa. PhD thesis, Nagoya university, Japon.

Thieblemont, D and Tegyey, M., 1994. Une discrimination géochimique des roches différenciées témoin de la diversité d'origine et de situation tectonique des magmas calco-alcalins. Comptes Rendus de l'Académie des Sciences Paris 319 (II), 87–94.

Toteu, S.F., Macaudiere, J and Dautel, D., 1990. Metamorphic zircons from Northern Cameroon; implication for the Pan-African evolution of Central Africa. Geologische Rundschau 79, 777-788.

Toteu, S.F., Van Schmus, W. R., Penaye, J., Michard, A., 2001.New U-Pb and Sm-Nd data from North-central Cameroon and its bearing on the pre-Panafrican history of central Africa. Precambrian Research 108, 45-73.

Toteu, S.F., Penaye,J., Poudjom Djomani, Y.H., 2004. Geodynamic evolution of the Pan-African belt in Central Africa with special reference to Cameroon. Canada Journal. Earth Sciences 41, 73-85.

Tack,L., Wingate, M.T.D., Liégeois,J.P., Fernandez-Alonso, M., Deblond, A.,2001. Early Neoproterozoic magmatism (1000–910 Ma) of theZadinian and Mayumbian Groups (Bas-Congo): onset of Rodinia rifting at the western edge of the Congo craton.Precambrian Research 110, 277–306.

Zindler, A and Hart, S.R., 1986.Chemical geodynamics. Ann. Rev.Earth Planet. Sci., 14, 493-571.